

Liversidge Research Lecture

No. 9
1952

ELECTRON DIFFRACTION IN THE CHEMISTRY OF THE
SOLID STATE

A. L. G. REES



The Royal Society of New South Wales



Albert Lloyd George Rees

Reproduced from a photograph in the collection of Dr. J.B. Willis

ALBERT LLOYD GEORGE REES 1916-1989

Albert Lloyd George (Lloyd) Rees was born in Melbourne on 15 January 1916. He was educated at Carey Baptist Grammar School 1924-1933, and graduated Dux of the School, having been Head Prefect and School Captain in his final year. His parents could not afford to send him to University, so in his last year at school Rees took the initiative of calling in to the Head Office of the Council for Scientific and Industrial Research (CSIR) to see Dr David Rivett who was then Chief Executive Officer of CSIR to ask about the possibility of working and doing a B.Sc. degree part-time. Rivett phoned Professor E.J. Hartung at the Chemistry Department, University of Melbourne, and in 1934 Rees began his course, working as a part-time laboratory assistant for Hartung.

Rees graduated B.Sc. with distinction in 1936 and took his M.Sc. degree in 1938, working under the supervision of Dr. N.S. (later Professor Sir Noel) Bayliss who earlier that year had been appointed to the Chair of Chemistry at the University of Western Australia, Perth. Because of a staff shortage there, Bayliss employed Rees as a temporary lecturer in organic chemistry for the first two terms of 1939. Rees then proceeded to London to take up a Beit Scientific Research Scholarship to work for his Ph.D. degree under Professor H.J. Emeleus. It was then war time, and as a contribution to the war effort Emeleus had undertaken to study war gases that might be used against the Allies by the enemy; Rees' project was concerned with the preparation and properties of arsine. He graduated Ph.D. in 1941, and then took a position with Philips Electrical Industries U.K. as leader of a new research and development group in their Materials Research Laboratory at Mitcham in Surrey. In late 1944 he returned to Australia to become leader of the newly created Section of Chemical Physics, within the Division of Industrial Chemistry of the Council for Scientific and Industrial Research (CSIR). This position he filled with great distinction and in 1958 he was appointed as Chief of the newly created separate Division of Chemical Physics within what had become (in 1949) the Commonwealth Scientific and Industrial Research Organisation (CSIRO); he held this position until his retirement in 1978.

Lloyd Rees was President of Section B (Chemistry) of ANZAAS in 1963, and President of the R.A.C.I. for the period 1967-68. His research was in various types of spectroscopy, including electron microscopy, electron diffraction, and the chemistry and physics of the defect solid state.

Honours and Awards

- 1945 Rennie Medal, Australian Chemical Institute
- 1948 Fellow, Australian Chemical Institute
- 1948 D.Sc., University of Melbourne
- 1951 Fellow, Australasian Association for the Advancement of Science (ANZAAS)
- 1951 H.G. Smith Medal, Royal Australian Chemical Institute (RACI)
- 1952 Liversidge Research Lecture, Royal Society of New South Wales

- 1954 FAA (a foundation Fellow of the Australian Academy of Science)
- 1970 Leighton Memorial Medal, RACI
- 1977 D. Appl. Sc., *honoris causa* , Victoria Institute of Colleges
- 1978 CBE (Commander of the British Empire)
- 1978 Lloyd Rees Library - CSIRO Division of Chemical Physics
- 1987 Ian William Wark Medallist and Lecturer - Australian Academy of Science
- 1989 Honorary Life Member - Australian Scientific Industry Association
- 1990 Lloyd Rees Memorial Lecture - Australian Academy of Science.

Biographical Sources

1. Willis, J.B., 'The Chemists of Australia: Dr. A.L.G. Rees', *Chemistry in Australia*, 1978, **45**, (6), 157-159.
2. Willis, J.B., 'The CSIRO Division of Chemical Physics', *Historical Records of Australian Science*, 1988, **7** (2), 153-177.
3. Walsh, A. and Willis, J.B., 'Albert Lloyd George Rees 1916-1989', *Historical Records of Australian Science*, 1992, **9** (1), 31-47.

Scientific Publications of A.L.G. Rees

The 77 scientific publications of Lloyd Rees are listed in an appendix to reference (3) given above under Biographical Sources.

**ELECTRON DIFFRACTION IN THE CHEMISTRY OF THE
SOLID STATE***

A. L. G. REES

*Chemical Physics Section, Division of Industrial Chemistry, C.S.I.R.O.,
Melbourne.*

Technical rather than scientific progress over the last 20 years has been largely responsible for the useful application of physics to the problems of chemistry. Naturally enough physical methods find immediate application in the identification and analysis of chemical species; later, as a proper understanding of the physical phenomenon is acquired, application to the more fundamental problems of structure, energetics and dynamics becomes possible. Electron diffraction has been understood fairly completely, in a formal way at least, from a time shortly after the establishment of wave mechanics, but recent experimental advances have only now permitted some realization of its full potential in chemistry.

The terms of the Liversidge Bequest require that the subject of this lecture should be such as to encourage research and stimulate interest in some aspect of chemistry. The importance of the chemistry of the solid state, both in academic and technological spheres, the relevance and uniqueness of the information on the solid state provided by electron diffraction and the prospect of exciting experimental and theoretical development constitute a topic which, I venture to submit, satisfies these terms.

The Electron Diffraction Method

Electrons, of mass m and charge e , accelerated by a potential V of the order of 50 kV., have, from the relation $\lambda = h / (2me V)^{1/2}$, an equivalent wave-length λ of $\sim 0.06 \text{ \AA}$, somewhat smaller than the normal X-ray wave-lengths used in diffraction studies, but still of the right order of magnitude for diffraction by regular arrangements of atoms or molecules. One would expect an electron diffraction pattern to have a formal resemblance to an X-ray diffraction pattern; this is so, but there are important differences. Indeed, it is these differences which represent the value of electron diffraction in chemistry. By reason of its charge a 50 kV. electron can penetrate only some hundred or so atomic planes without suffering considerable inelastic scattering (i.e., scattering in which kinetic energy of translation is not conserved). Moreover, electrons are scattered elastically by atoms some 10^7 times more efficiently than are X-rays. Electron diffraction is restricted then to the study of solid surfaces and of extremely small crystals, for both of which X-ray diffraction is of indifferent value.

Those refinements to the technique of electron diffraction responsible for widening its

* Liversidge Research Lecture delivered to the Royal Society of New South Wales, July 17, 1952. Reproduced by permission of the Royal Society of New South Wales from *J. Proc. Roy. Soc. N.S.W.*, 1952, **86**, 38-54.

scope have been largely electron-optical in character. An electron diffraction camera is simply an instrument for producing a narrow beam of high-velocity electrons by means of a system of electromagnetic lenses and small apertures, and recording on a photographic plate held normal to the beam direction the beams diffracted by the specimen. Figure 1 is a diagrammatic representation of the principle of a high-resolution electron diffraction camera.

For high resolution in single-crystal reflections, with which we shall be particularly concerned here, the electrons in the narrow pencil impinging on the specimen must be of uniform velocity, as this determines their wave length, and must have small angular spread. To fulfil these conditions stability in accelerating voltage (determining the electron velocity) and in lens current (determining the focal length of the lens) and freedom from external perturbations, either electrical, magnetic or mechanical, are required. For a given

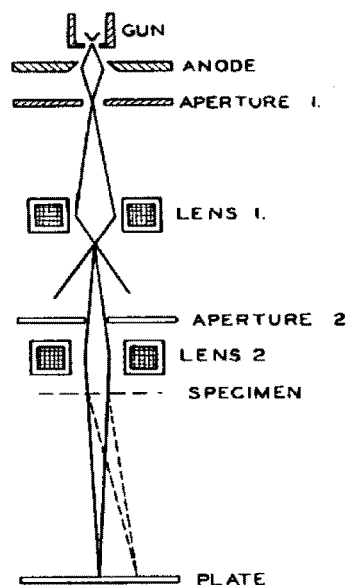


FIGURE 1. - Principle of high resolution electron diffraction camera.

resolution, the tolerable fluctuations in any of these may be calculated. This problem was analysed before construction of the diffraction camera in Melbourne (Cowley and Rees, 1952), which is shown in Plate I, Fig. 2.

Many of the applications of electron diffraction to solid-state studies require high resolution, since it is the fine structural detail of these patterns which provides the relevant information. Recent work indicates that experimental conditions must be controlled even more rigorously if all useful information is to be extracted from the method.

Diffraction patterns obtained from specimens in which the crystallites are in random orientation, either by transmission through a powder specimen or by reflection from the surface of a polycrystalline solid, consist of circles centred on the undeflected beam. The radii of the rings give the diffraction angle $2\theta_{hkl}$, related to the lattice spacings d_{hkl} by the Bragg law -

$$(2/\lambda) \sin \theta_{hkl} = 1/d_{hkl}$$

Patterns from a single crystal or from a number of crystals in identical orientation consist of single reflection spots or, in special cases, an array of spots, which has become known

as a cross-grating pattern owing to its resemblance to the diffraction pattern from a two-dimensional grating.

It is convenient to discuss diffraction from single crystals in terms of a concept introduced by Ewald, that of the *reciprocal lattice*. This concept is one of the most useful in diffraction studies; as it is necessary for subsequent discussion it will be outlined briefly here. The vector equivalent of Bragg's law is given by a construction wherein the incident beam is represented by a vector \vec{S}_0 , of magnitude $1/\lambda$ and the diffracted beam by a vector \vec{S}_1 , of identical magnitude but making an angle 2θ with the incident beam. The difference between the vectors \vec{S}_1 and \vec{S}_0 is a vector of magnitude $1/d_{hkl}$ if the diffraction condition is satisfied. All diffracted beam vectors must terminate on the surface of a sphere centred on the origin of the beam vectors and centred on the origin of the beam vectors and of radius $1/\lambda$. If d_{hkl} is a proper lattice spacing then it is obvious from Figure 3 that Bragg's law is implicit in this construction.

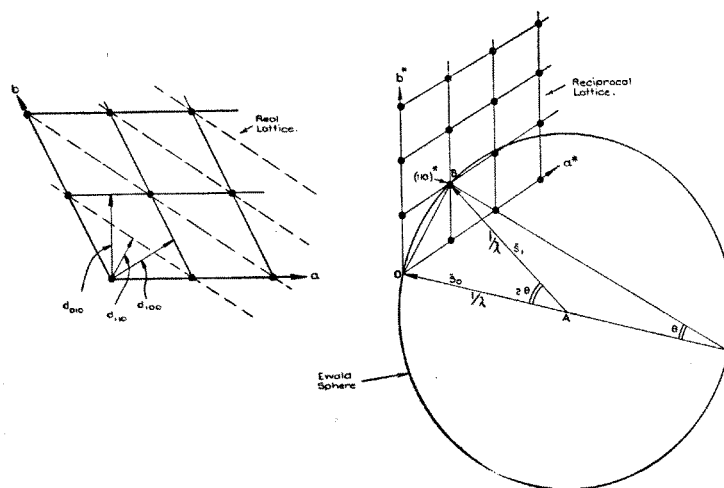


FIGURE 3. - Ewald's reciprocal-lattice construction for diffraction conditions.

The vector \vec{OB} , having the direction of a normal to the diffracting planes and of magnitude $1/d_{hkl}$ is termed a *reciprocal lattice vector*. For any given crystal lattice, a reciprocal lattice of terminal points of vectors $1/d_{hkl}$ may be constructed. The directions of the permitted diffracted beams for a specific orientation of the crystal to the incident beam vector \vec{AO} will then be given by the vectors \vec{AB} terminated at the intersections of the Ewald sphere and the integer points of the reciprocal lattice. A change in orientation of the real crystal leads to a rotation of the reciprocal lattice about its origin O through the same angle. In this way different integer points of the reciprocal lattice intersect the surface of the Ewald sphere and diffracted beams are permitted. Reflections for which $1/d_{hkl}$ is greater than $2/\lambda$ will not be permitted as the corresponding reciprocal lattice points lie outside the volume swept out by the Ewald sphere pivoted on O.

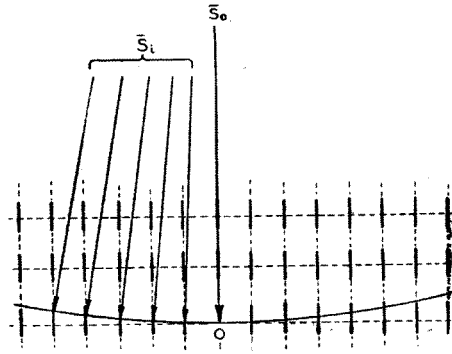


FIGURE 4. - Reciprocal-lattice construction for diffraction by a thin crystal plate. Electron beam parallel to short dimension of crystal.

In the same way that the resolving power of an optical diffraction grating is determined by the total number of lines, the angular breadth of a reflection from a three-dimensional crystal grating is greater the smaller the number of scattering points in the crystal. For an *infinite crystal* the reciprocal lattice is a lattice of points and the angular range of any reflection is infinitesimal; for a *finite crystal* the deterioration in resolution appears in the reciprocal lattice as a spreading of each reciprocal lattice point. This spread will be greatest in the direction of the smallest dimension of the crystal. The Ewald sphere will now pass through the region around a reciprocal lattice point for a range of directions of the incident beam vector. This is the origin of the dependence of breadth of reflections on crystal size.

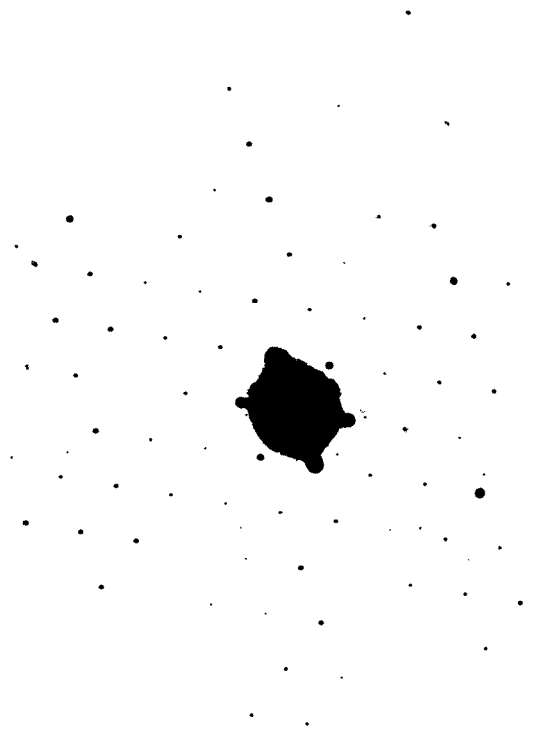


FIGURE 5. - Cross-grating pattern from crystal of boric acid.

The construction for the diffraction of fast electrons is simplified as $1/\lambda$ is much greater than the unit reciprocal lattice spacings and the Ewald sphere may be approximated by a plane or near-plane sectioning the reciprocal lattice. Moreover, since the small penetration of electrons limits the effective dimensions of the three-dimensional grating, it is to be expected that reciprocal lattice points will be invariably extended into the space between the integer points. For a thin crystal plate the diffraction conditions are as shown in Figure 4. The reciprocal lattice points are drawn out into spikes parallel to the short dimension of the crystal and the Ewald sphere of large radius can section many of these spikes simultaneously. The pattern resulting from such a diffraction experiment is a cross-grating pattern, a symmetry-true projection of a section of the reciprocal lattice. An example of such a pattern is given in Figure 5.

The Structural Problem

Application of electron diffraction to chemical problems followed its discovery very promptly; particularly successful applications came from the laboratories of G. I. Finch, G. P. Thomson, S. Kikuchi, J. J. Trillat and L. H. Germer (Thompson and Cochrane, 1939; Finch and Wilman, 1937). Studies of the growth and structure of thin films, of the structure of metal oxides, particularly surface oxides, of surface films and lubrication were among the important fields of application to chemistry. The useful fundamental information extracted from these investigations was confined to cell dimensions, crystal symmetry, orientation and habit, and to some extent structure. No structural problems were attempted from single-crystal data and Fourier methods were not applied. The reason for this lay in the anomalies in observed electron diffraction intensities and in the presence of reflections forbidden on space-group grounds. These anomalies were ascribed to various causes, among them dynamic interaction, limitation of crystal dimensions and secondary scattering.

Over the last five years Pinsker and his colleagues (Vanchstein and Pinsker, 1949, 1950) have used intensity data from powder patterns to analyse crystal structures by Fourier methods. The disadvantage of using patterns of this type, from which only one parameter, the Bragg angle, is available for determining the geometry of the lattice and in which different reflections often appear in coincidence, is familiar to all crystallographers. The possible use of single crystal data for structure analysis was examined in Melbourne several years ago as the result of the study of secondary scattering of electrons (Cowley *et al.*, 1951a).

The high efficiency of elastic scattering of electrons results in the appearance of a considerable proportion of the incident energy in the diffracted beams; strong primary reflections may therefore be rediffracted by underlying crystallites or mosaic elements of the same crystal as shown in Figure 6. This secondary scattering may lead to many unusual and anomalous features in patterns; in polycrystalline specimens extra spots, extra rings, groups of spots, diffuse bands with sharp edges and rings centred on primary spots may occur; in single-crystal patterns a redistribution of the intensity among the reflections in the pattern and the appearance of the forbidden reflections may result. These features are illustrated in the patterns as shown in Plate II, Figs. 7, 8, 9 and 10.

In the cross-grating pattern of Plate II, Fig. 10, there are superimposed secondary patterns identical with the primary pattern and of the same orientation, but centred on each of the primary reflections. The secondary reflections consequently coincide with primary reflections of different indices. This is illustrated in Figure 11. Each reflection in the

pattern has lost intensity by contributing to all other reflections and has gained by secondary contributions from every other spot. This modification of the intensities is the obstacle to their use for structure analysis.

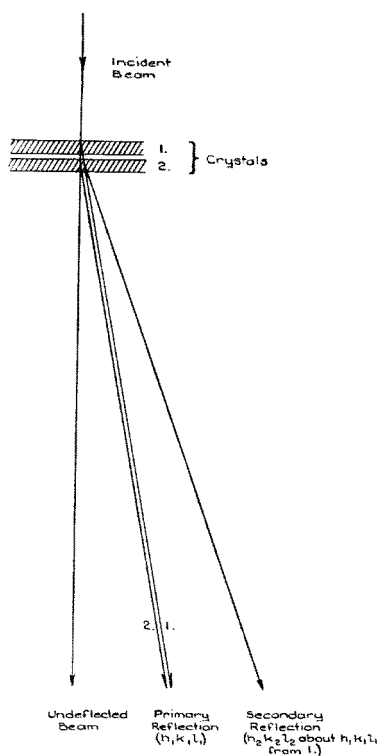


FIGURE 6 - Diagrammatic representation of secondary elastic scattering of primary diffracted beams by underlying crystallites.
See Plate II, Figs. 7-10.

The theoretical problem is relatively simple. The contribution by secondary scattering from a reflection $h_1k_1l_1$ to another reflection $h_2k_2l_2$ is proportional to the product of the theoretical intensities

$$I_{h_1k_1l_1} \cdot I_{(h_2+\bar{h}_1)(k_2+\bar{k}_1)l_2}$$

and the total contribution from all primary reflections to this reflection is proportional to the sum of such products over all indices h_1 and k_1

$$\sum_{h_1} \sum_{k_1} I_{h_1k_1l_1} \cdot I_{(h_2+\bar{h}_1)(k_2+\bar{k}_1)l_2}$$

A mathematical analysis on this basis leads to an expression for the correction of observed intensities for secondary scattering. The magnitude of the corrections and the way in which they account for the intensity anomaly is shown in Figure 12. The importance of this correction in structure analysis was tested by obtaining basal-plane Fourier projections of the hydrocarbon dicytyl ($C_{32}H_{66}$). The Fourier projections obtained from diffraction of electrons are projections of the distribution of potential in the lattice and not of the electron density, to which, however, they are closely related. In Figure 13 the contour map obtained from uncorrected intensities shows spurious and misleading detail; in Figure 11

the contour map obtained from corrected intensities not only shows the carbon atom positions but also gives an indication of the hydrogen atom positions.

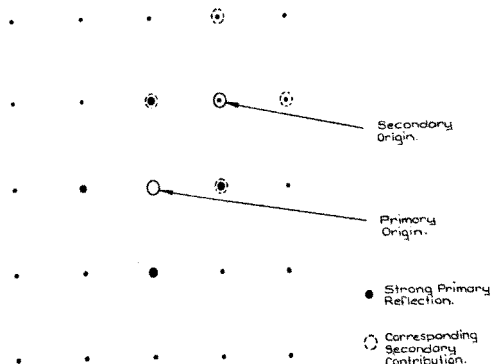


FIGURE 11.- Diagram showing coincidence of secondary reflections with primary reflections of different indices in a cross-grating pattern.

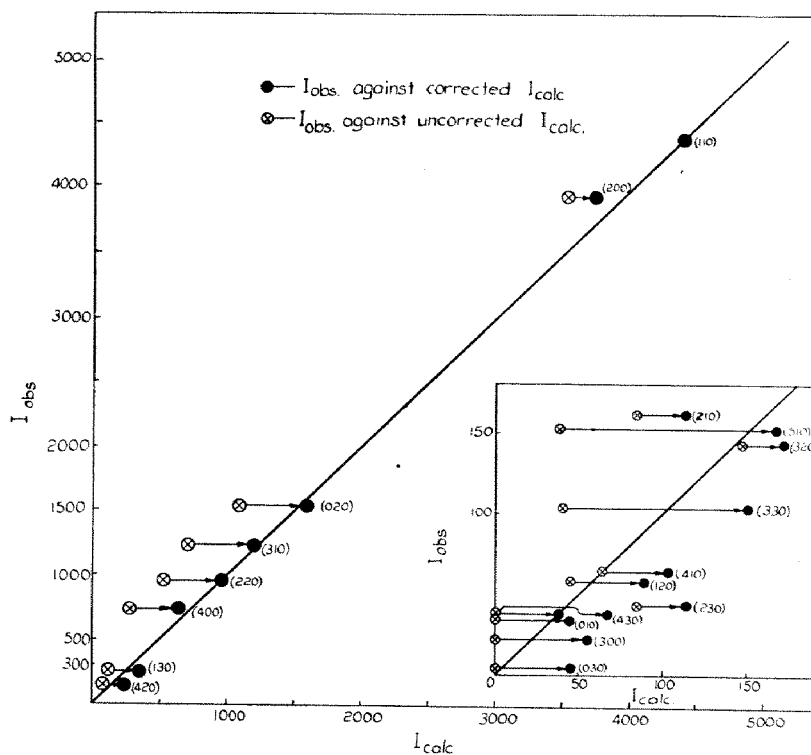


FIGURE 12 - Comparison of observed and calculated intensities of reflections from dicetyl single-crystal. Satisfactory correspondence of observed and calculated intensities is obtained only when a correction for secondary scattering is introduced.

Fig. 13.

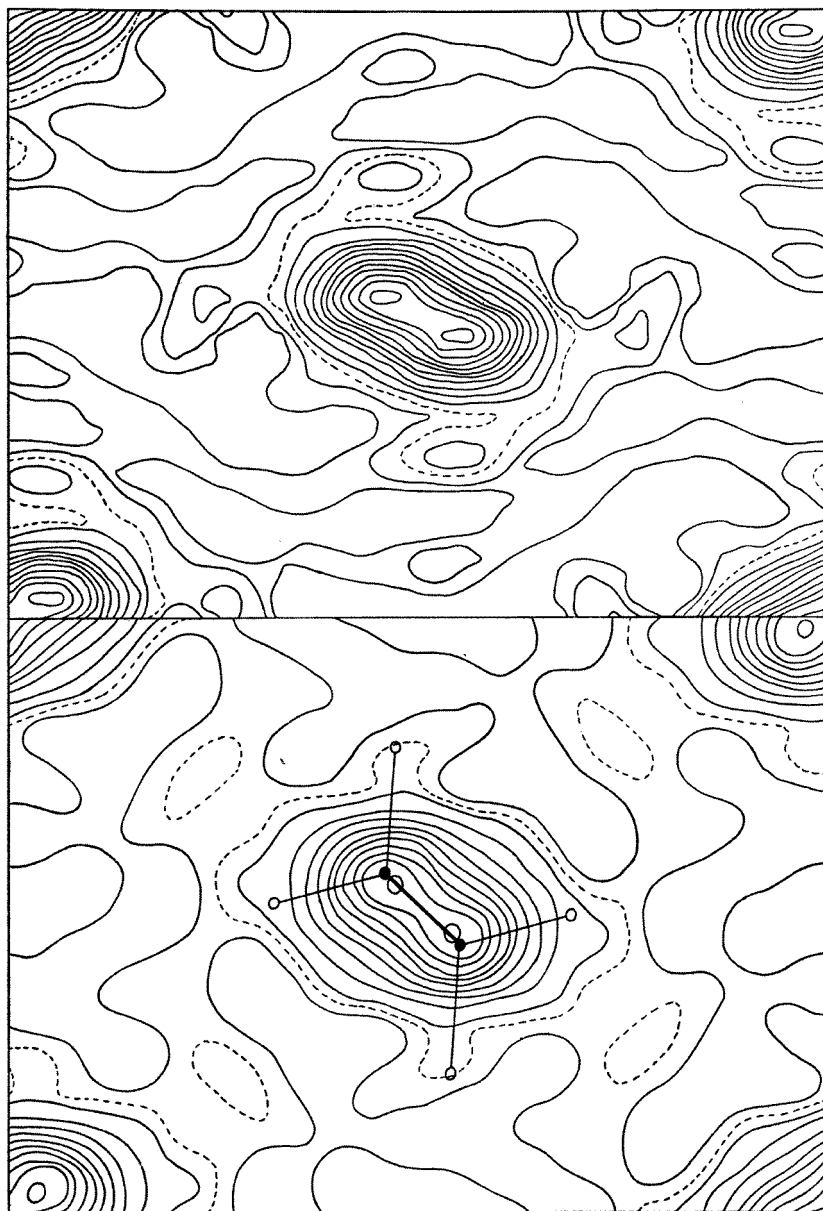


FIGURE 13. Basal-plane Fourier projection of potential distribution in dicetyl using intensity data uncorrected for secondary scattering.

FIGURE 14. Basal-plane Fourier projection of potential distribution in dicetyl using intensity data corrected for secondary scattering. Full circles denote carbon atom positions and open circles hydrogen atom positions deduced from data on bond lengths and angles. Note that the hydrogen atom positions are clearly indicated in the contour map.

This particular test structure analysis made it clear that the application of electron diffraction to structural problems in chemistry had specific merit. Crystals of very small dimensions only are necessary and light atoms, notably hydrogen, can be located more readily than by X-ray methods owing to their higher relative scattering power for electrons than for X-rays. New problems are, however, introduced, a major one being the measurement of intensities. Intensities must be measured with greater accuracy than in the X-ray method, but this is not difficult to achieve.

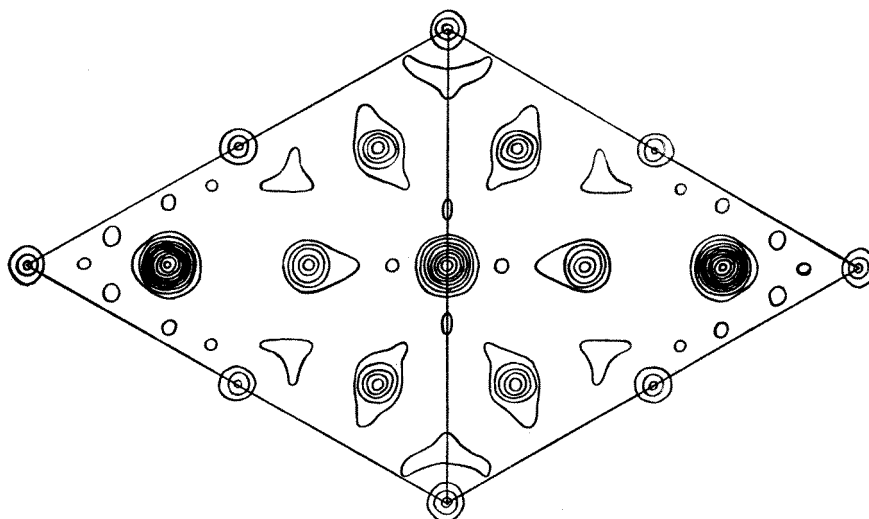


FIGURE 15. (111)-Fourier projection of γ - Al_2O_3 obtained from intensities in an electron diffraction cross-grating pattern. This projection must be interpreted in terms of a stacking disorder in the lattice.

The results of subsequent structural studies by Dr. J. M. Cowley and Mr. A. F. Moodie have justified development of this method and illustrate its value in chemistry.

It has been known for some time that the electron diffraction pattern of polycrystalline gold foil developed several extra reflections if the specimen was heated at $\sim 500^\circ\text{C}$ in air or oxygen. Nothing of this sort occurred if larger specimens treated in the same way were studied by X-ray methods. Moodie (unpublished work) succeeded in obtaining cross-grating patterns after protracted heating of gold films in oxygen and was able to identify several Au-O phases of different symmetry from these patterns. The intensity data were complete enough to obtain Fourier projections of two of these phases. The significant feature of this result is that gold dissolves oxygen to form well-characterized phases of low oxygen content, even though on a bulk specimen this may be confined to a surface layer less than 100 \AA thick. This is, moreover, a problem which could not be investigated by X-ray methods as the low heat of formation of these phases and the high heat of activation of the diffusion of oxygen into gold preclude the preparation of any but a small amount of the material in a reasonable time.

Cowley (unpublished work) has studied the structure of γ -alumina and related compounds. A (111) Fourier projection of a disordered γ - Al_2O_3 (cubic, spinel-type) is shown in Figure 15. The X-ray work on γ - Al_2O_3 has been confined to powder patterns largely because of the small crystal size and the extensive disorder.

The structure of boric acid has been determined by Zachariassen (1934) by X-ray methods in so far as the boron and oxygen locations are concerned, but no information on the location of the hydrogen atoms was obtained. It was inferred from the intermolecular O-O distances, however, that hydrogen-bonds occur extensively in the structure. Cowley (1952) has developed new methods of dealing with stacking disorder in layer-lattice structures and has been able to obtain a clear projection of a single two-dimensional atom layer showing trigonal BO_3^{3-} groups and also the *hydrogen bonds* interlinking these groups. The projection is shown in Figure 16. It is to be noted that (i) the hydrogen atom in the bond tends to be near either one oxygen or the other and not symmetrically disposed

between them, and (ii) hydrogen positions do not lie on the internuclear line between the hydrogen-bonded oxygens. Evidently the explanation is to be found in the interaction of the two parallel orthodox hydrogen bonds. There are, in fact, eight different canonical structures that may be written down showing different possible positions of the protons. These structures are given in Figure 17 together with the resultant distribution. This type of hydrogen-bond "resonance" must be common among oxyacids of the non-metals and probably occurs in protein structures also. This type of structural study would certainly be impossible by X-ray methods at present.

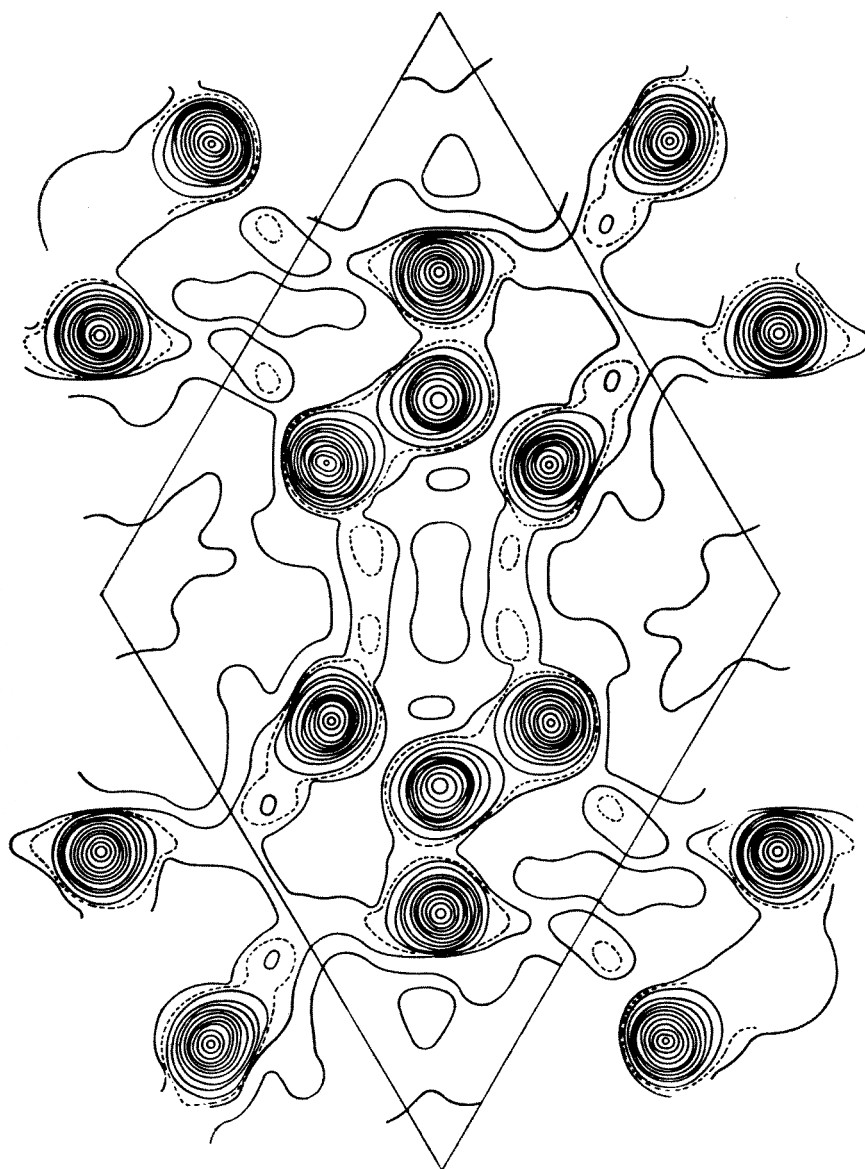


FIGURE 16. Basal-plane Fourier projection of boric acid crystal showing distribution of potential in single two-dimensional layer of the lattice. The trigonal groups are BO_3^{3-} , each forming three pairs of hydrogen bonds with the three neighbouring BO_3^{3-} groups. Note the distribution of potential in the region of the hydrogen-bond pairs.

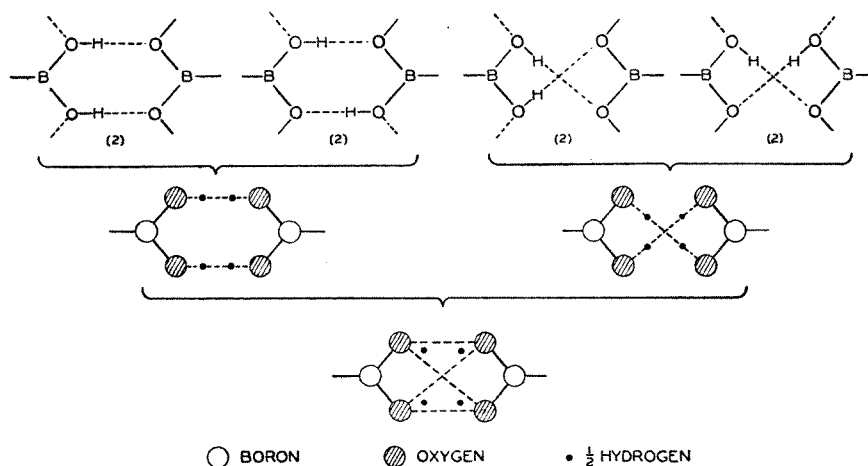


FIGURE 17. Diagram showing the eight possible canonical structures for a pair of hydrogen bonds in the boric acid structure and the resulting "resonance" structure.

Of further chemical interest is the fact that structural disorder is common in small crystals. For layer-lattice structures it is invariably present. It is possible that the 3-dimensional structure of larger crystals is not the thermodynamically stable configuration when crystal dimensions are small. Moreover, there is evidence (Rees and Spink, 1950*a*) that the lattice parameters change significantly when crystal dimensions are reduced. Further study along these lines is desirable.

Fine Structure in Electron Diffraction Patterns and the Size and Habit of Crystals

High-resolution diffraction patterns show fine structure of the individual single-crystal reflections which is closely related to the size and habit of the crystal. The origin of this fine structure is to be found in two effects, namely (i) the deviation of an electron beam on crossing a crystal boundary (refraction) (Sturkey and Frevel, 1945; Hillier and Baker, 1945, 1946; Cowley and Rees, 1946, 1947; Honjo, 1947), and (ii) the extension of reciprocal lattice points arising from small crystal dimensions (Rees and Spink, 1950*b*). These effects may be discussed independently by means of a kinematic approximation, adequate for most purposes, or more rigorously by a dynamic treatment.

Since the potential inside a crystal is different from that of free space, the electron velocity is also different and a refraction phenomenon is to be expected. Actually the square root of the inner potential is the electron analogue of the refractive index for light. Angular deviation of an electron beam will occur at the entrant and exit faces of a crystal and also, if the diffraction conditions are satisfied, at the diffracting planes inside the

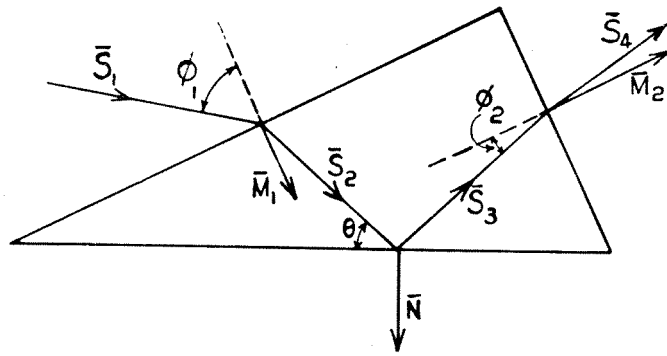


FIGURE 18. Diagram of deviation of an electron beam at entrant and exit faces of a crystal at diffraction plane.
 \bar{S}_1 , \bar{S}_2 , \bar{S}_3 , and \bar{S}_4 are beam vectors; \bar{M}_1 and \bar{M}_2 are crystal normals;
 \bar{N} is the diffracting plane normal; θ is the Bragg angle.

crystal, as shown in Figure 18. Since the deviations due to refraction are normally very small, electrons entering non-parallel faces of the crystal may still satisfy the somewhat relaxed diffraction conditions associated with small crystals. Each single reflection will consequently be broken up into a number of components corresponding to the number of possible entry and exit faces presented to the beam by the crystal in its given orientation. Typical spot groups attributable to refraction are shown in Plate III, Fig. 19. The spot configuration is characteristic of the orientation and habit of the crystal.

The effect of crystal shape can be discussed only in terms of the reciprocal lattice. As we have seen earlier, the shape of the relevant reciprocal lattice region about an integer

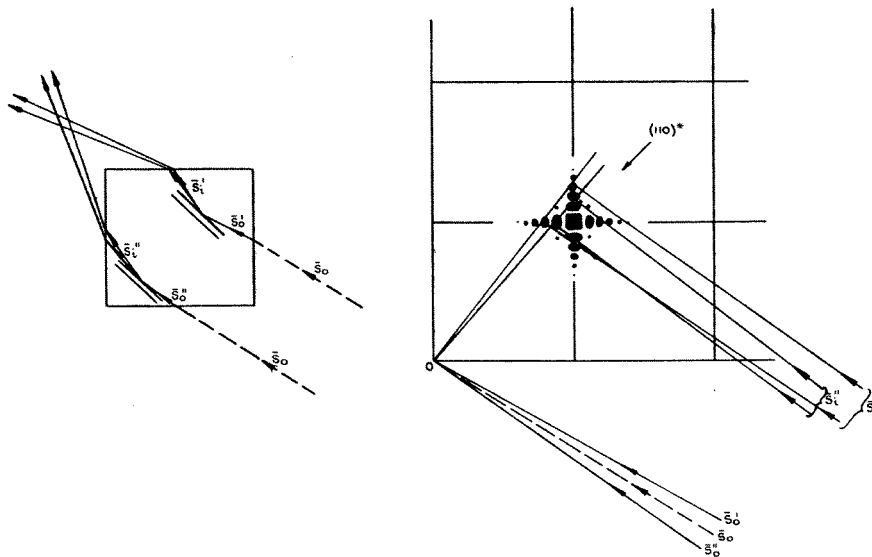


FIGURE 20. Diagram illustrating splitting of the 110 diffraction spot into group of reflections by a very small crystal of regular habit (cubic) in real and reciprocal space.

The vectors \bar{S}_0 denote beams prior to diffraction, the vectors \bar{S}_1 denote beams after diffraction.

The distribution of scattering amplitude (square of the shape transform) around the $(110)^*$ reciprocal-lattice point is shown on a considerably enlarged scale.

point depends on the external form of the crystal and in fact the distribution of scattering amplitude around each integer point of the reciprocal lattice is accurately described by the square of a function of the reciprocal lattice co-ordinates known as the shape transform. This amplitude is greatest along directions perpendicular to crystal faces and the transform is in fact a 3-dimensional periodic function. For a plain parallel slab the scattering amplitude is extended along the c^* -direction and is of the form $\sin^2 N\pi u / (N\pi u)^2$, where u is the reciprocal lattice co-ordinate measured from the integer point and N is the number of scattering points in that direction. Referring now to Figure 20, in which the situation for refraction and diffraction at (110) planes of a small crystal of cubic habit is represented in real and reciprocal space, we see the way in which the more complicated spot groups originate. A contour map of the distribution of scattering amplitude around a reciprocal lattice point in a small crystal of cubic habit is shown in Figure 21.

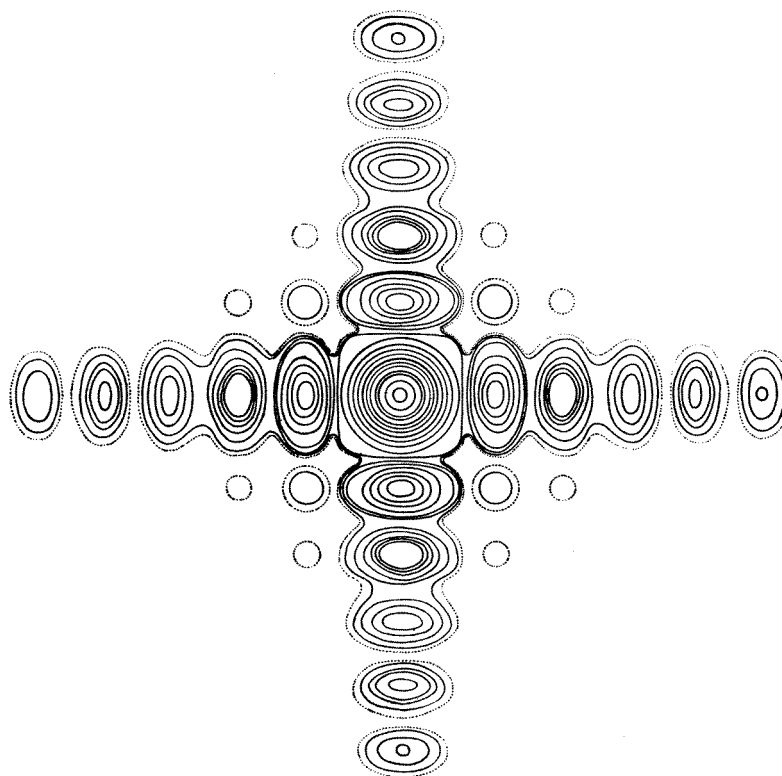


FIGURE 21.- Contour map of scattering amplitude around a reciprocal lattice point for a crystal of cubic habit.

There is now a different Ewald sphere for each face of entry and each sphere makes a different section of the amplitude function. Each refraction spot is broken up into a configuration determined by the shape transform. In some instances the sphere sections the transform in such a way as to show the subsidiary maxima, from the positions of which the dimensions of the crystallite may be determined uniquely (Rees and Spink, unpublished). Examples of this are shown in Plate I, Fig. 22. Further development of this could provide one with a powerful method of studying crystal growth.

An interesting example is provided by zinc oxide prepared by burning zinc in air or oxygen. The particles grow as "fourlings", four elongated hexagonal prisms roughly in tetrahedral configuration. Often one finds thin sheets forming webs between one spine and each of the other three. Further spines may grow from these sheets. It has been possible to use electron diffraction methods to provide a complete morphological description of these crystals (Cowley *et al.*, 1951*b*). A drawing of an idealized crystal is shown in Figure 23

and an electron micrograph in Plate III, Fig. 24. The reason for this fantastic habit is not known, but it does represent an interesting problem in the mechanism of crystal growth.

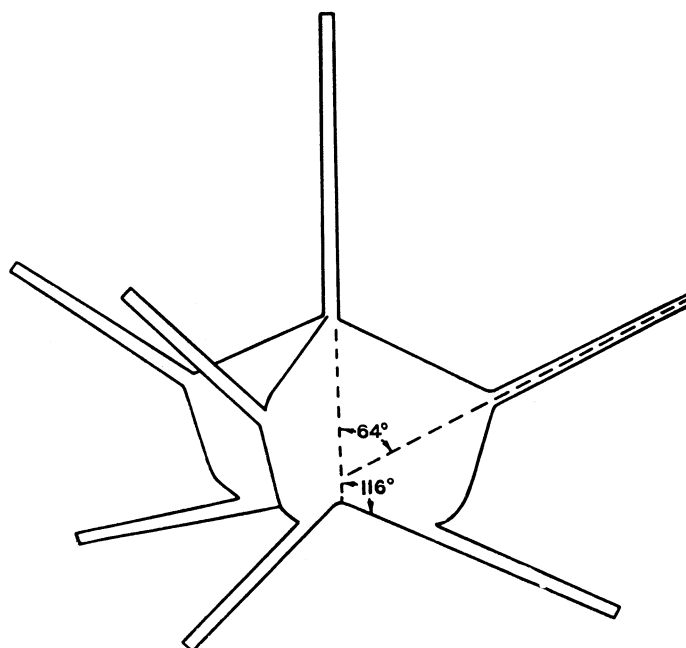


FIGURE 23.- Diagram of ideal crystal form of "fourling" in ZnO smoke. Three needles of hexagonal section are twinned on $(11\bar{2}2)$ with the fourth needle (vertical in the diagram) making an angle of 116° with it. The webs grow as continuations of the lattice of the vertical needle and have a twin relationship with the three lower needles.

The possibility of deducing the shape of the molecules of crystalline proteins is within reach. These molecules are well ordered units of dimensions of the order of 50-100 Å and should give reflections from individual molecules in a dried molecular dispersion. The water necessary to preserve long-distance order in protein crystals is intermolecular and drying should not therefore interfere with the order in each individual molecule. Shape transform detail should allow a complete and unique description of the polyhedral shape of the molecule to be given, an important step in the structure analysis of large complex molecules.

The rigorous (dynamic) treatment of diffraction (Bethe, 1928; Heidenreich, 1950; and Kato, 1951) predicts a different effective inner potential for different reflections, a prediction which is confirmed by experiment. Experimental data on the dimensions and configurations of spot groups such as those of Figure 19 may be used to deduce the Fourier coefficients V_{hkl} of the three-dimensional potential distribution in the unit cell. Goodman (unpublished work) has been able to compute the V_{hkl} values for several reflections in MgO from his experimental data and has shown that they are in good agreement with values obtained from the known structure of MgO. This provides us with a new approach to structure analysis. The Fourier coefficients may be determined for all observable reflections by measurements of spot group dimensions and the structure analysis performed in the usual way. This could be of considerable value for crystals for which intensity measurements are difficult to make. It is my opinion that this represents the most promising approach to the problem of structure analysis by electron diffraction.

Reactions in the Solid State

At some stage in a reaction involving the solid state a new solid phase must be formed from a solid reactant phase. The mechanism by which this is accomplished is a problem of some importance in chemistry. For simplicity we may examine two types of solid-state reactions, namely

- (i) *tarnish reactions*, in which an oxide, sulphide, halide, etc., film is formed on the surface of a metal by reaction with the corresponding non-metallic element ; and
- (ii) *simple dissociation processes*, in which an ionic compound is decomposed by thermal or photo-chemical means into a gas and a solid product.

The nucleation and growth steps are always the result of aggregation of defects in the crystal, *e.g.* in simple dissociation reactions the step may be either the aggregation of interstitial cations or of vacant anion lattice sites trapping electrons. A schematic representation of the aggregation of vacancy defects is given in Figure 25. The aggregate of defects is in fact simply a lattice of cations and electrons, that is, a small crystal of the metal with somewhat enlarged lattice dimensions and perhaps different symmetry. It is clear that the defect aggregate will at some point become thermodynamically unstable and break away from the parent lattice to form a small crystal of the metal of correct lattice dimensions. The metal lattice will have an orientational relationship to the parent lattice which will reflect the mechanism of nucleation and this can be established by electron diffraction studies. Moreover, the size and shape of the precipitated particles can be deduced from the fine structure.

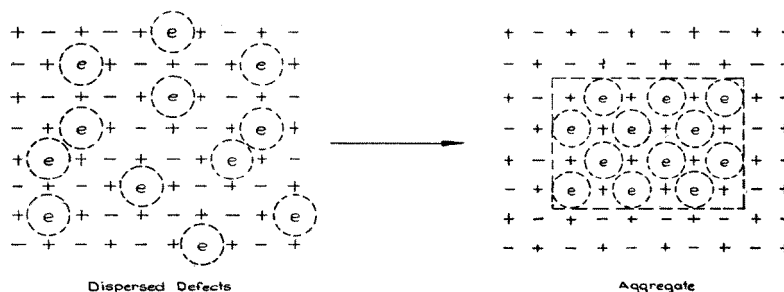


FIGURE 25. - Illustration of the aggregation of F-centre defects in an ionic lattice to give a metallic nucleus.

An illustration of this type of study is Pashley's (1950, 1951) recent work on the photolytic and electron-induced decomposition of silver halides. Pashley was able to show that the lattice of silver produced from silver chloride is in parallel orientation to the silver chloride lattice, even though the cell dimensions of the two are such that no good atomic fit is to be expected. AgCl is a cubic crystal of the NaCl type; the Ag⁺ ions form a face-centred cubic lattice of side 5.55 Å. Removal of Cl⁻ ions by aggregation of F-centre defects will leave a face-centred lattice of Ag of side 5.55 Å, which at some stage collapses to give the face-centred cubic lattice of silver metal of side 4.08 Å without change of orientation. This particular study is of importance in the mechanism of the photographic process. Reactions in the solid state are intimately associated with the existence of crystal defects, the structural consequences of which are almost unknown. In my opinion electron diffraction is capable of providing this information with little improvement on present experimental methods.

Conclusion

Our understanding of the chemistry of the solid state, particularly those aspects which concern small crystals and defect solids, is still elementary and any prospect of increasing this understanding is of no small consequence. Recent developments in electron diffraction show promise of improving this knowledge and point the way to undoubtedly fertile fields of scientific work.

The work we have done in Melbourne in an effort to pioneer some of these fields has been carried out by a small group, namely Dr. J. M. Cowley, Messrs. A. F. Moodie, P. Goodman and J. A. Spink. They are responsible for the diffraction patterns used for illustration here, and I gratefully acknowledge my indebtedness to them.

References

- Bethe, H.A., 1928. *Ann. Physik*, **87**, 55.
Cowley, J.M., 1952. *Nature*. (In press.)
Cowley, J.M., and Rees, A.L.G., 1946. *Nature*, **158**, 550.
1947. *Proc. Phys. Soc.*, **59**, 287.
1952. *J. Sci. Instr.* (In press.)
Cowley, J.M., Rees, A.L.G., and Spink, J.A., 1951a. *Proc. Phys. Soc.*, **A 64**, 609.
1951b. *Proc. Phys. Soc.*, **B 64**, 638.
Finch, G.I., and Wilman, H., 1937. *Ergebn. exakt. Naturw.*, **16**, 353.
Heidenreich, R.D., 1949. *J. Appl. Phys.*, **20**, 993.
1950. *Phys. Rev.*, **77**, 271.
Hillier, J., and Baker, R.F., 1945. *Phys. Rev.*, **68**, 98.
1946. *J. Appl. Phys.*, **17**, 12.
Honjo, G., 1947. *J. Phys. Soc. Japan*, **2**, 133.
Kato, N., and Uyeda, R., 1951. *Acta Crystallographica*, **4**, 227, 229.
Pashley, D.W., 1950. *Acta Crystallographica*, **3**, 163.
1951. "Fundamental Mechanisms of Photographic Sensitivity",
Butterworth, London, p. 39.
Rees, A.L.G., and Spink, J.A., 1950a. *Nature*, **165**, 645.
1950b. *Acta Crystallographica*, **3**, 316.
Sturkey, L., and Frevel, L.K., 1945. *Phys. Rev.*, **68**, 56.
Thomson, G.P., and Cochrane, W., 1939. "Theory and Practice of Electron Diffraction",
Macmillan, London.
Vanshstein, B.K., and Pinsker, Z.G., 1949. *J. Phys. Chem., U.S.S.R.*, **23**, 1058.
1950. *Dokl. Akad. Nauk., S.S.S.R.*, **72**, 53.
Zachariasen, W., 1934. *Z. Krist.*, **88**, 150.

PLATE I

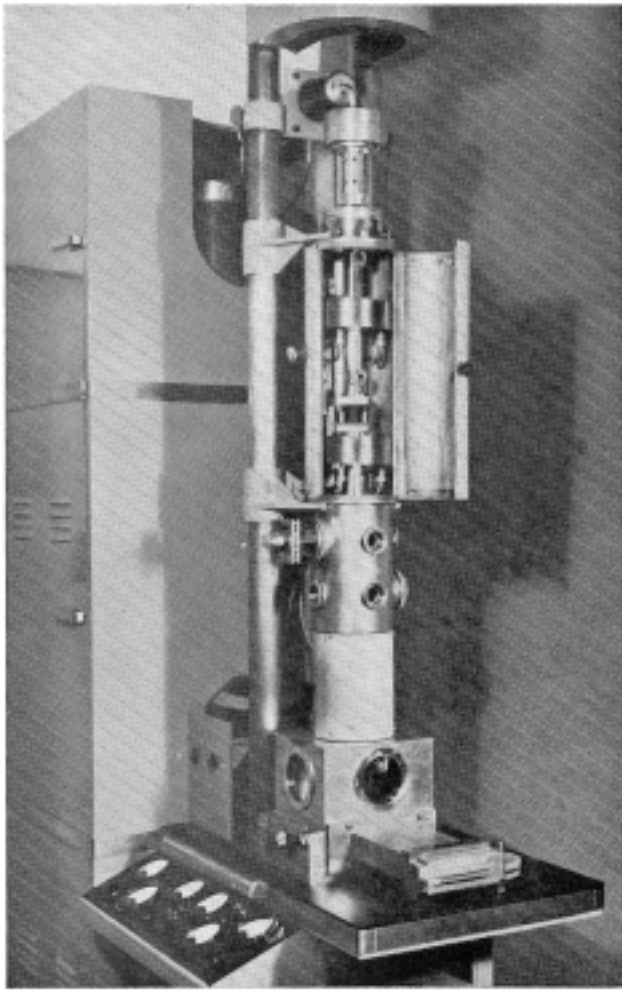


Fig. 2.

Fig. 2. Electron diffraction camera in Chemical Physics Section, Division of Industrial Chemistry, C.S.I.R.O., Melbourne.

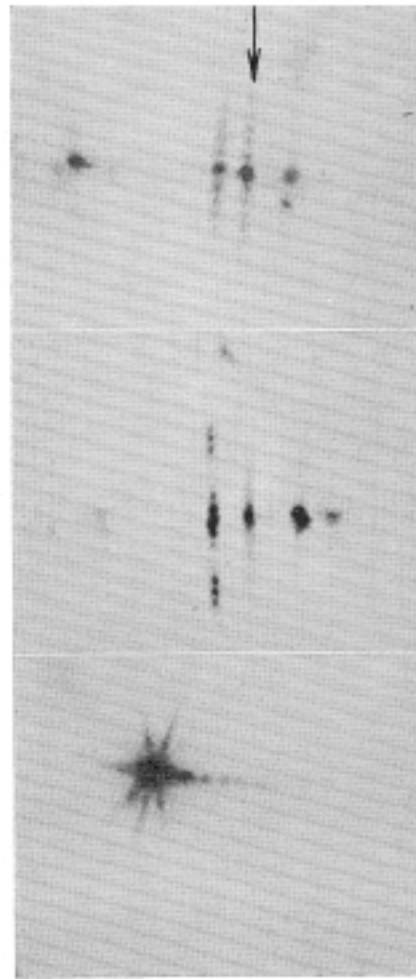


Fig. 22.

Fig. 22. Fine structure of single reflections in patterns from small crystals of ZnO of elongated hexagonal prismatic habit.

PLATE II

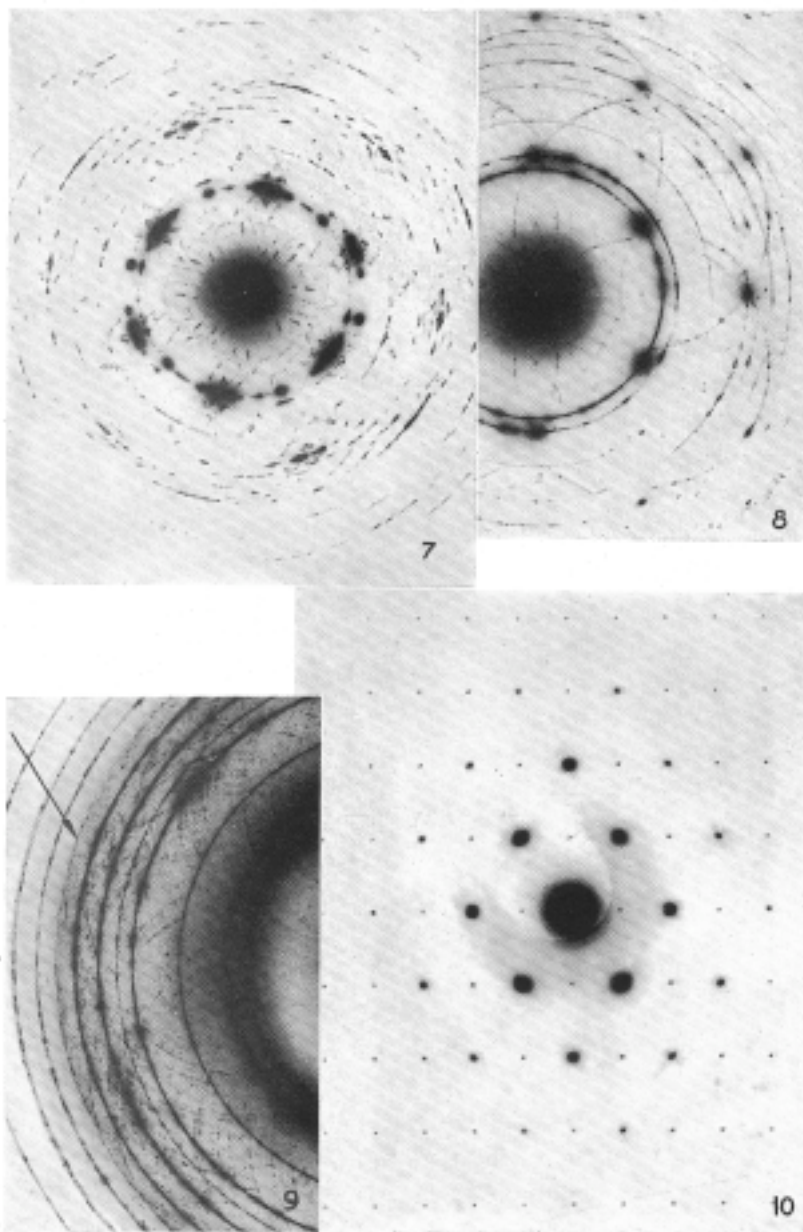


Fig. 7. Electron diffraction pattern from crystals of a long-chain paraffin hydrocarbon. Secondary scattering is responsible for diamond-shaped groups of reflections and extra spots inside first strong ring.

Fig. 8. Electron diffraction pattern from dicetyl showing secondary rings centred on strong primary reflections. Secondary rings originate from diffraction by numerous small crystals in random orientation underlying a large crystal giving the strong primary spots.

Fig. 9. Electron diffraction pattern from dicetyl illustrating the origin of "extra" rings. The envelope (distinguished by an arrow) of the numerous secondary rings, which originate from either (i) 200 secondaries around 110 primaries, or (ii) 110 secondaries around 200 primaries, forms a non-legitimate "extra" ring centred on the undeflected beam.

Fig. 10. Cross-grating pattern from single-crystal of dicetyl showing effects attributable to secondary scattering. The odd orders on both axes are forbidden on space-group grounds, but appear in the pattern as a result of secondary scattering.

PLATE III

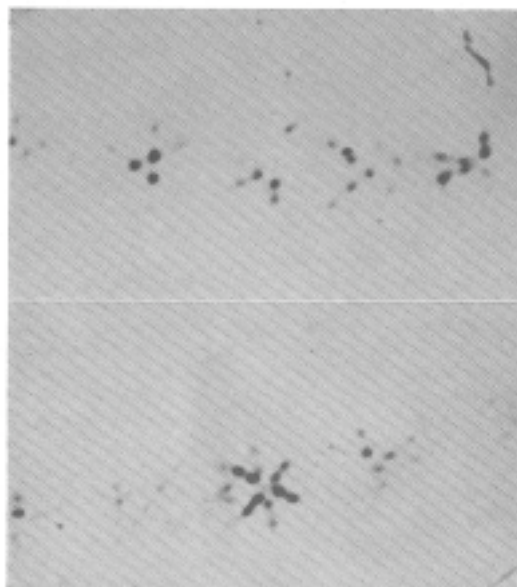


Fig. 18.

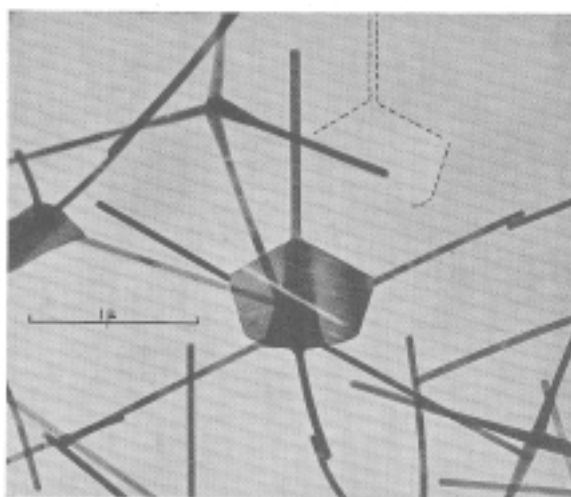


Fig. 24.

Fig. 19. Typical spot groups in patterns from MgO crystals of cubic habit. These spot groups, which comprise the fine structure of ring patterns from specimens consisting of randomly oriented crystals of regular habit, are attributable in part to refraction effects.

Fig. 24. An electron micrograph of an imperfect ZnO "fourling" showing webs. The dotted outline is a dark-field image of this crystal.